Axin proteolysis by Iduna is required for the regulation of stem cell proliferation and intestinal homeostasis in *Drosophila*

Yetis Gultekin[1] and Hermann Steller[1]*

[1]Strang Laboratory of Apoptosis and Cancer Biology, The Rockefeller University, 1230 York Avenue, New York, NY 10065, USA.

***Corresponding author:**

E-mail: steller@rockefeller.edu. Strang Laboratory of Apoptosis and Cancer Biology, The Rockefeller University, 1230 York Avenue, New York, NY 10065, USA. Tel: (212) 327-7075.

Running Title: Iduna regulates stem cell proliferation and intestinal homeostasis

Keywords: protein degradation, ubiquitin proteasome system, Wingless, Axin, JAK-STAT, ADP-ribosylation, Tankyrase, Iduna, stem cells, *Drosophila*.

Abstract

The self-renewal of intestinal stem cell is controlled by Wingless/Wnt-β catenin signaling both in *Drosophila* and mammals. Axin is a rate-limiting factor in wingless signaling. Hence, its regulation is essential. Iduna is an evolutionarily conserved ubiquitin E3 ligase that has been identified as a critical regulator of degradation of ADP-ribosylated Axin and thus of Wnt-β catenin signaling. However, its physiological significance remains to be demonstrated. Here, we generated loss-of-function mutants of *Iduna* and investigated its physiological role in the *Drosophila* midgut. Genetic depletion of *Iduna* causes the accumulation of both Tankyrase and Axin in *Drosophila* cells. Increase in Axin protein in enterocytes non-autonomously enhanced stem cell divisions. Enterocytes secreted Unpaired and thereby stimulated the activity of the JAK-STAT pathway in intestinal stem cells. A decrease in *Axin* gene expression suppressed both the over-proliferation of stem cells and restored their numbers to normal levels in *Iduna* mutants. These findings suggest that Iduna-mediated regulation of Axin proteolysis is essential to maintain tissue homeostasis in the *Drosophila* midgut.

Introduction

The evolutionarily conserved Wnt/β-catenin signaling pathway is a main regulator of animal development. It controls proliferation, differentiation and regeneration of adult tissues (Nusse and Clevers, 2017). The Wingless pathway is also involved in adult tissue self-renewal in *Drosophila* (Lin et al., 2008). Genetic depletion of proteins in the Wingless pathway, such as *Tcf*, *arr, dsh* and *pygo,* leads to inhibition of Wingless signaling activation which in turn causes over-proliferation of stem cells in the *Drosophila* midgut (Kramp et al., 2002; Wang et al., 2016a and 2016b; Tian et al., 2016). However, inactivation of Wnt signaling in the small intestine of mice decreases the proliferative potential of stem cells (Fevr et al., 2007; Korinek et al., 1998). On the other hand, mutations which result in over-activation of the Wnt-β catenin cascade promote tumorigenesis (Clevers and Russe, 2012; Andreu et al., 2005; Korinek et al., 1997 and 1998; Morin et al., 1997). For instance, mutations on *adenomatous polyposis coli (APC)* gene cause a hereditary colorectal cancer syndrome called familial adenomatous polyposis (Kinzler et al., 1991; Nishisho et al., 1991). Axin loss-of-function mutations are found in hepatocellular carcinomas, while oncogenic β-catenin mutations are described in colon cancer and melanoma (Rubinfeld et al., 1997). Consequently, intense efforts have been made to target this pathway for therapeutic purposes (Clevers and Russe, 2012).

A key feature of the Wnt/β-catenin pathway is the regulated proteolysis of the downstream effector β-catenin by the β-catenin degradation complex. The principal components of this complex are adenomatous polyposis coli (APC),

Axin and Glycogen synthase kinase 3α/β (GSK3α/β) (Hamada et al., 1999; Salic et al., 2000; Lee at al., 2003). Axin, a critical scaffold protein in the β-catenin degradation complex, is the rate-limiting factor of Wnt signaling and its protein levels are regulated by the Ubiquitin Proteasome System (UPS) (Li et al., 2012). Axin is targeted for degradation by the combined action of the poly-ADP-ribose polymerase Tankyrase (TNKS) and the ubiquitin E3-ligase Iduna/Ring finger protein 146 (RNF146) (Zhang et al., 2011). Both genetic and pharmacological studies suggest that UPS-dependent degradation of Axin occurs in a specific temporal order. Iduna initially exists in an inactive state, but binding to its iso- or poly-ADP-ribosylated targets causes allosteric activation of the enzyme (DaRosa et al., 2015). Hence, in the initial step, TNKS binds to Axin and ADP-ribosylates Axin by using NAD^+. Then, Iduna recognizes and binds to ADP-ribosylated Axin via its WWE domain and poly-ubiquitylates Axin. Following the ADP-ribosylation and ubiquitination, post-translationally modified Axin is rapidly degraded by the proteasome (DaRosa et al., 2015; Wang et al., 2016a and 2016b; Croy et al., 2016; Callow et al., 2011). This tight control suggests an important function for Iduna to regulate the Wnt-β catenin pathway.

Since the stability of Axin is partially regulated by TNKS-mediated ADP ribosylation, specific small-molecule inhibitors have been developed to inhibit Wnt-sigaling (Lu et al., 2009; Huang et al., 2009). For example, XAV939 targets the ADP-ribose polymerase activity of TNKS and increases Axin levels, which in turn destabilizes β-catenin to inhibit Wnt signaling (Huang et al., 2009). There are two TNKS isoforms in mammalian cells (Hsiao et al., 2006). *Tnks1*$^{-/-}$ and *Tnks2*$^{-/-}$

mice are overall normal; however, double knock-out of *Tnks1/2* causes early embryonic lethality, which indicates their redundancy in mouse development (Hsiao et al., 2006; Chiang et al., 2008). On the other hand, inactivation of the single *Drosophila Tnks* gene produces viable flies that have slightly increased Axin levels but no overt defects (Wang et al., 2016a and 2016b; Feng et al., 2014; Yang et al., 2016; Tian et al., 2016). Therefore, the exact physiological function of TNKS and Iduna-mediated regulation of Wnt-signaling remains to be determined. In order to address this question, we generated and characterized *Drosophila* Iduna loss-of-function mutants and demonstrate a critical function of this pathway for stem cells in the *Drosophila* intestinal tract.

The *Drosophila* genomes encode four isoforms of *CG8786/Iduna/RNF146*, which is evolutionarily conserved from *Drosophila* to human. In this study, we concentrated on the physiological function of Iduna in the adult *Drosophila* midgut, which shares several striking similarities with the mammalian small intestine but offers greater anatomical and genetic accessibility (Micchelli et al., 2005; Ohlstein et al., 2005; Markstein et al., 2013). Under normal conditions, Wingless signaling controls stem cell proliferation and cell fate specification in adult midgut (Tian et al., 2016). Here, we show that Iduna has a physiological function to regulate the proteolysis of both TNKS and Axin. Inactivation of *Iduna* results in increased numbers of midgut stem cells and progenitors due to over-proliferation. We find that Axin accumulation in enterocytes promotes the secretion of Unpaired, a cytokine that binds to the Domeless receptor and activates the JAK-STAT pathway in stem cells and thereby promotes stem cell

division. Significantly, reducing *Axin* expression by half restores the numbers of ISC. These findings indicate that regulation of Axin proteolysis by Iduna is necessary to control intestinal homeostasis in *Drosophila*.

Results

Iduna plays a role in Axin degradation: To examine the *in vivo* function of *Drosophila* Iduna, CRISPR-Cas9 genome editing was used to generate *Iduna* mutants. *Iduna* is located on the 3rd chromosome of *Drosophila*. We designed a specific guide RNA that targets *Iduna*`s first exon and identified two mutant alleles by Sanger sequencing: $Iduna^{17}$ and $Iduna^{78}$, which have 4-nucleotides and 2-nucleotides deletions, respectively (Fig 1A). These deletions are close to the translation start side of *Iduna*. Next we assessed the levels of mRNA and protein expression in these mutants. Using reverse transcript PCR analysis, we found significantly reduced amounts of *Iduna* transcripts in the $Iduna^{78}$ mutant. On the other hand, were unable to detect any *Iduna B* and *C/G* transcripts in the $Iduna^{17}$ allele (Fig 1B). Moreover, no Iduna protein was detected in either of these mutants, indicating that they represent Null-mutations (Fig 1C). Finally, genetic analyses of these alleles in trans to a larger deletion (see below) indicate that both alleles are complete loss-of-function mutations.

Iduna mutants were crossed to *Drosophila* deficiency lines [Df(3L)Exel6135, Df(3L)ED228)] and also to each other and all combinations were viable as trans-heterozygotes. *Iduna*-Null flies had no overt morphological defects when compared with wild type controls. However, *Iduna* mutants displayed increased mortality under reduced nutrient conditions (Fig 1D).

Iduna is one of the key components of the machinery that degrades Axin whose ADP-ribosylation by TNKS is important for mammalian Wnt-β catenin signaling (Li at al., 2012). To understand the contribution of *Iduna* inactivation for both

TNKS and Axin proteolysis in *Drosophila*, UAS-Flag-TNKS and UAS-GFP-Axin transgenes were expressed under an eye-specific driver, *GMR-Gal4*, in an *Iduna* mutant background. Five day-old adult male heads were lysed and total proteins were analyzed by immunoblotting to detect the levels of tagged proteins (Fig 1E and G). *Iduna* mutants had 2.5-fold more Axin protein when compared to wild type (Fig 1F). These mutants had 3.5-fold more TNKS protein as well (Fig 1G-H). Therefore, Iduna can promote the proteolysis of both Axin and TNKS.

Iduna is required to control the proliferation of intestinal progenitors in the *Drosophila* midgut: Wingless signaling is required to control intestinal stem cell proliferation in *Drosophila* (Xu et al, 2011; Cordero et al., 2012; Tian et al., 2016). Since *Iduna* mutants have elevated Axin level and increased mortality upon starvation, we hypothesized that *Iduna* inactivation may cause defects in the digestive system. Just as the mammalian intestine (Korinek et al., 1998), the *Drosophila* midgut has intestinal stem cells (ISCs), which give rise to all intestinal compartments (Micchelli et al., 2005; Ohlstein et al., 2005). ISC are marked by the expression of a transcription factor, *escargot (esg),* whose GFP reporter allows tracing of stem and progenitor cells during development (Ohlstein et al., 2005) (Fig 2A-B). Using the *esg>GFP* marker, we saw an approximately twofold increase in the numbers of ISCs/progenitors in the midgut of *Iduna*-Null mutants compared to controls (Fig 2C-D).

ISCs give rise to two types of daughter progenitor cells: undifferentiated enteroblasts (EBs) and pre-enteroendocrine cells (Pre-EE). EBs and pre-EEs differentiate into enterocytes (ECs) and enteroendocrine (EEs) cells, respectively

(Ohlstein et al., 2005; Xu et al., 2011) (Fig 1SA-B). *Iduna* inactivation increased the numbers of $Arm^+/Pros^-$ cells (Fig 2E-F) approximately twofold compared to controls (Fig 2G-H). We also observed a slight increase in the total cell number in the midgut of *Iduna* mutants (Fig 2SA). On the other hand, there were no significant differences in the number of EC and EE cells (Fig 2SB-D). Collectively, these observations indicate that *Iduna* inactivation leads to elevated numbers of ISCs in the *Drosophila* midgut.

The observed increase in ISC-numbers could be the result of aberrant stem cell proliferation or inhibition of their differentiation. To distinguish between these possibilities, we first assessed cell proliferation (Fig 3A-B). Using EdU-labelling, we observed that *Iduna* mutants had more EdU-positive cells (Fig 3C). Moreover, phospho-Ser-Histone H3 (pH3) immunostaining (Fig 3D-E) also revealed a significant increase in $pH3^+$ mitotic cells in the midgut of *Iduna*-Null mutants (Fig 3F). These findings suggest that ISCs undergo increased proliferation in *Iduna* mutants. To address the second possibility whether there was inhibition of differentiation in *Iduna* mutants, we generated mutant clones (Theodosiou et al., 1998). We found that ECs and EEs were present in the mutant clones, demonstrating that Iduna was not essential for differentiation of ISCs to daughter cells (Fig S2A-H).

Regulation of Axin proteolysis by Iduna is necessary for normal ISC proliferation: In order to determine the function of *Iduna* in the *Drosophila* midgut in more detail, we investigated the consequences of *Iduna* inactivation on Axin in this system. For this purpose, we first expressed a UAS-GFP-Axin

transgene under the enterocyte specific temperature sensitive *Myo1A-Gal4* driver (Fig 4A). Using this reporter, we saw 2-2.5 fold more Axin in *Iduna* mutants compared to controls (Fig 4B).

Mammalian Iduna recognizes both ADP-ribosylated (ADPR) TNKS and Axin via the R163 residue in its WWE domain (Zhang et al., 2011). The R163 residue is conserved in evolution and corresponds to R252 in the *Drosophila* WWE domain (Fig 4C). To examine the level of ADPR-Axin in *Iduna* mutants, endogenous ADPR-Axin was pulled down with recombinant wild type or R252A-WWE-mutant proteins (Fig 4D). This analysis revealed that *Iduna* mutants had a more than two-fold increase in ADPR-Axin in their midgut compared to wild type (Fig 4E). Finally, *Iduna* mutant clones had more GFP-Axin when compared to neighboring cells (Fig 4F).

One plausible mechanism by which Iduna may control the proliferation of ISCs in the *Drosophila* midgut is through modulating the concentration of Axin. To determine whether a reduction of the elevated Axin levels could reduce ISC numbers in *Iduna* mutants, they were recombined with *Axin* mutants and then crossed again with *Iduna* mutants to generate flies that were homozygous mutant for $Iduna^{(-/-)}$ and heterozygous for $Axin^{(+/-)}$. Strikingly, a reduction of the *Axin* gene dosage by 50% restored ISC numbers to wild type levels in *Iduna* mutants (Fig 5A). Compared to normal controls, *Iduna* mutants had an approximately twofold increase in the number of $Arm^{+}/Pros^{-}$ as well as $pH3^{+}$ mitotic stem cells (Fig 5B-C). On the other hand, reducing the *Axin* gene dosage by 50% in an *Iduna*-Null background yielded numbers of ISCs and the $pH3^{+}$ stem cells comparable to wild

type. These results suggest that small changes in the levels of Axin have profound effects on stem cell number, and that regulation of Axin degradation by Iduna is necessary to for normal ISC proliferation.

The proliferation of ISCs in the *Drosophila* midgut is regulated by intrinsic signals and also interactions with neighboring cells (Zhou et al., 2013; Tian et al., 2016). To further investigate whether the observed effects reflect a cell-autonomous requirement of Iduna in stem cells, or alternatively a requirement in other cells of the midgut, *Iduna* was specifically targeted in enterocytes as well as the midgut stem cells and progenitors by using *Myo1A-Gal4* and *esg-Gal4* drivers, respectively (Fig 6A). RNAi-mediated knock-down of *Iduna* in enterocytes caused a significant increase in stem cell numbers (Fig 6B). However, stem cell/progenitor cell-specific knock-down of *Iduna* did not affect either the stem cell numbers or mitosis in midgut (Fig 6B-C). This suggests that *Iduna* inactivation causes ISC over-proliferation by a non cell-autonomous mechanism, and that perhaps enterocytes are responsible for stem cell over-proliferation in *Iduna* mutants. To further test this idea, we ectopically expressed Iduna in enterocytes and investigated if this could suppress stem cell proliferation in *Iduna* mutants (Fig 6D). Indeed, consistent with this model, we saw that *Myo1A-Gal4* driven UAS-Iduna was able to restore normal numbers of stem cells and progenitors (Fig 6E-F). Taken together, our results indicate that Iduna plays a physiological role to regulate Wingless signaling in enterocytes, which is critical for proper ISC proliferation.

Depletion of *Iduna* promotes stem cell proliferation through the JAK-STAT pathway: In order to further investigate the mechanism by which Iduna affected ISC proliferation, we explored the function of additional signaling pathways implicated in this system. Because the JAK-STAT pathway has a well-known role in stem cell proliferation (Zeidler et al., 2000; Zoranovic et al., 2013; Zhou et al., 2013; Markstein et al., 2013), we looked for possible effects of *Iduna* mutants here. Using a STAT-GFP reporter line (Bach et al., 2007), we saw that stem cells were the STAT-GFP$^+$ cells (Fig 7A) and *Iduna* mutant clones had elevated JAK-STAT signaling (Fig 7B). To test whether activation of JAK-STAT signaling was responsible for aberrant ISC proliferation, we knocked down *stat92E*, a transcription factor in the JAK-STAT pathway, in enterocytes as well as in stem cells and progenitors. Interestingly, knock-down of *stat92E* in ISCs was sufficient to suppress their increased proliferation in *Iduna* mutants (Fig 7C). Collectively, these observations suggest that *Iduna* inactivation causes abnormal Wingless signaling in enterocytes, which in turn causes elevated JAK-STAT signaling in ISCs and thereby results in their over-proliferation.

This model raises the question of how enterocytes signal ISC proliferation. One possibility is that enterocytes secrete a factor activating the JAK-STAT pathway in ISCs. The JAK-STAT pathway can be activated by cytokines, such as unpaired (UPD, UPD2, UPD3) in *Drosophila* (Ghiglione et al., 2002; Zhou et al., 2013). Therefore, we explored the possibility that unpaired cytokines mediate ISC over-proliferation in *Iduna* mutants. For this purpose, we first inactivated *Iduna* under *Upd3-Gal4* driver and found that RNAi-mediated knock-down of

Iduna resulted in a significant promotion of *Upd3>UAS-GFP* reporter (Fig 7D). We then reduced *Upd2* and *Upd3* expression by 50% in *Iduna* mutants (Fig 7E). Strikingly, we observed that a 50% reduction in *Upd2-Upd3* expression fully suppressed ISC proliferation in *Iduna* mutants (Fig 7E). Secreted Unpaired proteins bind to the Domeless receptor on ISCs (Ghiglione et al., 2002). Hence, our model predicts that decreasing Domeless levels should also suppress ISC cell over-proliferation in *Iduna* mutants. Again, this prediction was experimentally confirmed (Fig 7E). We conclude that inactivation of *Iduna* causes abnormal Wingless signaling in enterocytes, which in turn leads to increased secretion of UPD2-3 from these cells to stimulate over-proliferation of ISCs through the JAK/STAT pathway (Fig 7F).

Discussion

In this study, we investigated the *in vivo* function of *Iduna* in the control of stem cell proliferation in the *Drosophila* midgut. It was previously shown that mammalian Iduna is an unusual E3-ubiquitin ligase that specifically binds to and poly-ubiquitylates ADP-ribosylated substrates to promote their rapid degradation by the proteasome. However, the physiological function of Iduna remains largely unclear. In this study, we generated *Drosophila* Null-mutants and used them to show that Iduna has a critical *in vivo* function for the degradation of ADP-ribosylated TNKS and Axin to control stem cell proliferation. In particular, we focused on the role of *Iduna* in the *Drosophila* midgut. We found that *Iduna* inactivation caused a slight but significant increase in Axin protein levels in enterocytes, which in turn caused over-proliferation of intestinal stem cells. This non-cell autonomous effect on stem cell proliferation was depended on UPD2-UPD3 cytokines that are secreted from enterocytes. These findings suggest a model in which loss of Iduna function, which decreases Wingless pathway activity due to elevated Axin levels in enterocytes, which in turn causes increased secretion of UPD2-3 resulted from these cells to activate the JAK-STAT pathway in ISCs. Importantly, a 50% reduction in *Axin* gene dosage blocked the over-proliferation of stem cells in *Iduna* mutants, demonstrating the necessity to tightly regulated Axin levels in this system. Whereas many other cell types appear to tolerate fluctuations in the amount of Axin protein, proper Wingless signaling in the *Drosophila* midgut appears to critically depend on restricting Axin levels by Iduna.

The activity of Iduna depends on binding to ADP-ribosylated substrates via its WWE domain. Recognition and binding to its ADP-ribosylated target proteins changes the structural confirmation of Iduna. Subsequently, Iduna is activated to ubiquitylate its targets for proteasome-mediated degradation. It was previously reported that TNKS forms a tight complex with Iduna to control the proteolysis of target proteins (DaRosa et al., 2015). We could not detect any obvious morphological differences between *Iduna* mutants and wild type. Although this may seem somewhat surprising, it is consistent with inactivation of *Tnks* in *Drosophila,* which also causes no overt abnormalities (Feng et al., 2014; Wang et al., 2016a and 2016b; Yang et al., 2016). Like for *Iduna*, *Tnks* mutants have no obvious effects on wing development and the expression of *Wingless* target genes in larval wing discs, despite the fact that Axin levels are increased (Feng et al., 2014; Wang et al., 2016a and 2016b; Yang et al., 2016). Our interpretation of these findings is that most tissues can tolerate relative modest (2-3fold) changes of Axin. For example, it appears that a greater than 3-fold increase of endogenous Axin is required for functional consequences of altered Wingless signaling in *Drosophila* embryos (Yang et al., 2016) and 3-9-fold changes are needed in wing discs (Wang et al., 2016a). On the other hand, the *Drosophila* midgut appears much more sensitive to reduced Wingless signaling.

These results reveal the physiological importance of *Iduna* for Wingless signaling in the *Drosophila* midgut and have implications for the regulation of this highly conserved pathway in mammals. For example, conditional inactivation of *Iduna* in mouse bones leads to increased numbers of osteoclasts and inflammation

(Matsumoto et al., 2017a). In this system, down-regulation of *Iduna* leads to accumulation of Axin1 and 3BP2. This in turn attenuates β-catenin degradation and activates SRC kinase, respectively, thereby promoting the release of inflammatory cytokines in the bone (Matsumoto et al., 2017a). On the other hand, *Iduna* depletion reduces proliferation of osteoblasts and promotes adipogenesis in the mouse skeleton (Matsumoto et al., 2017b). Despite the obvious differences between mammalian bone and the *Drosophila* midgut, both systems show overall striking similarities in the use of TNKS/Iduna to restrict Axin levels to achieve proper levels of Wnt/β-catenin signaling during tissue homeostasis. Finally, our study also indicates that Axin may have a more general function as a scaffold protein to recruit multiple proteins which permit crosstalk with other pathways to modulate Wnt/β-catenin signaling.

Figure Legends

Figure 1: Loss-of-function mutants of *dIduna* are viable and increase TNKS and Axin protein levels. A- Scheme for generation of *Iduna* loss-of-function mutants via CRISPR-Cas9 genome editing in *Drosophila.* sgRNA against Iduna was designed to generate small nucleotide deletions, close to its translation initiation site. The three nucleotides were highlighted with red to indicate the location of Cas9 cleavage site. **B-** *Iduna* loss-of-function mutants $Iduna^{17}$ and $Iduna^{78}$ were isolated by Sanger sequencing. Deletions of 4 and 2 nucleotides, respectively, introduced early stop codons and led to truncations of Iduna protein. $Iduna^{17}$ had no detectable *dIduna* transcripts, and $Iduna^{78}$ had severely reduced *Iduna* mRNA based on RT-PCR. 7-day old adult females were analyzed for expressions of *Iduna*, *Ribosomal protein 49* (a house keeping gene) and *Ornitate aminotransferase* **C-** $Iduna^{17}$ and $Iduna^{78}$ have no detectable protein. Endogenous Iduna protein was detected by immunoblotting. Anti-dIduna antibody was generated in guinea pigs and 20 μg total protein lysates of 7d-old adult females were analyzed by immunoblotting. β-actin was used as a loading control. Both Iduna alleles have no detectable protein and behave genetically as Null-alleles. **D-** *Iduna* mutants display increased mortality under reduced nutrient conditions. 5-day old mutant or wild type females were kept on 5% sucrose diet. Mutant flies died within 17 days while 80% of wild type flies were still viable at this time. n=100 from each genotype. **E-** *Iduna* inactivation leads to increased Axin protein levels. A UAS-GFP-Axin reporter transgene was expressed under *GMR-Gal4* driver in the *Iduna* mutants or wild type. Iduna mutants had 2.5-fold

increased Axin protein. **F-** Quantification of GFP-Axin. Results are based on two repeats of independent replicates and Axin protein levels were normalized to β-actin. **G-** TNKS protein accumulates in *Iduna* mutants. A UAS-Flag-TNKS reporter transgene was expressed under the *GMR-Gal4* driver in *Iduna* mutants or wild type. **H**- Iduna mutants have increased TNKS protein. 5-day old adult male heads were dissected and 20μg of total protein lysates were analyzed by immunoblotting to assess the levels of GFP-Axin or Flag-tagged TNKS using α-GFP or α-flag antibodies, respectively. Western blot quantification was performed based on two independent experimental replicates, and protein levels were normalized with β-actin. Oregon R flies were used as a wild type control. Iduna mutants had 3.5-fold increased levels of TNKS. $p<0.001$ is indicated as ***.

Figure 2: *Iduna* mutants have increased numbers of intestinal stem cells and progenitors in their midgut. A-B- Inactivation of *Iduna* promoted the proliferation of the esg-GFP labelled progenitor cells in the *Drosophila* midgut. Intestinal stem and progenitor cells were visualized with a *esg>GFP* reporter construct. Posterior midguts were analyzed by confocal microscopy following anti-GFP and DAPI staining. **C-** Quantification of esg>GFP$^+$ stem cells and progenitors from adult flies of indicated genotypes. **D-** In wild type, 25-30% of posterior midgut cells were stem cells, as assessed by *esg>GFP* expression. On the other hand, 55-60% of the total cell population in *Iduna* mutants expressed the stem marker esg>GFP, representing a greater than two-fold increase. **E-F-** *Iduna* mutants had more Arm$^+$/Pros$^-$ intestinal stem cells in the *Drosophila* midgut. ISCs and enterocytes were distinguished by their cell size, high level of

membrane-associated Armodillo, and lack of nuclear Prospero staining. In contrast, small-sized differentiated enteroendocrines were recognized by nuclear Prospero staining. Posterior midguts were analyzed by confocal microscopy following staining for anti-Armadillo, Prospero and DAPI. **G-H** Quantification of $Arm^{+}/Pros^{-}$ ISCs from adult flies of indicated genotypes. The midguts of 7d-old adult females were dissected and analyzed by confocal microscopy. For the consistency, posterior midgut R5 region was analyzed in this study. $Iduna^{17/+}$ flies were used as control. n>12 from each genotype. *p<0.001* was indicated as *** and *p<0.0001* was marked as ****.

Figure 3: *Iduna* inactivation enhances proliferation of intestinal stem cells. A-B- Genetic depletion of *Iduna* leads to over-proliferation of intestinal stem cells in the midgut. EdU was used as a proliferation marker and administrated for 1h at 25^{0}C. 7-day old mutants or wild type female flies were dissected for analysis. Following fixation, EdU incorporation was analyzed by confocal microscopy. **C-** Increased numbers of EdU^{+} stem cells were seen in *Iduna* mutants, indicating increased cell proliferation. Posterior midguts were analyzed for quantification. **D-E-** *Iduna* mutants display elevated phospho-Ser-Histone 3 (pH3)-positive ISCs**.** **F-** Iduna inactivation leads to an increase of $pH3^{+}$ mitotic stem cells in the midgut. Quantification of $pH3^{+}$ proliferating cells was done in the whole midgut. n>12 from each genotype. *p<0.0001* was marked as ****.

Figure 4: *Iduna* inactivation results in increased Axin protein levels in the midgut. A- *Iduna* mutant midguts had elevated Axin protein. Midguts of 7d-old adult females, which were expressing GFP-Axin under the temperature sensitive

Myo1A-Gal4 driver, were dissected, lysed and analyzed by GFP immunoblotting. *Iduna* mutants had more Axin protein compared to the wild type. 20μg total intestinal lysates were analyzed by GFP immunoblotting and α-tubulin was used as a loading control. **B-** Loss-of-*Iduna* resulted in 2.2-fold GFP-Axin accumulation in the midgut. Western blot quantification was performed based on two independent experimental replicates, and protein levels were normalized to α-tubulin. **C-** Iduna recognized ADP-ribosylated (ADPR) Axin via the R252 residue of its WWE domain. This residue corresponds to R163 in the mammalian Iduna ortholog and is conserved during evolution. Recombinant wild type and R252A mutants were used as biochemical sensors to pull down the ADPR-Axin from *Drosophila* midguts. Myc-tagged WWE proteins were expressed and purified from *Drosophila* S2R+ cells by immuno-precipitation. **D-** Inactivation of *Iduna* leads to accumulation of ADPR-Axin. Wild type myc-tagged-WWE protein pulled down ADPR-Axin. In contrast, the R252A mutant did not interact with modified Axin. Following IP, eluted proteins were analyzed with an α-PAR antibody. The 50kDa heavy chain IgG is indicated on the blot. **E-** *Iduna* inactivation results in 2.3-fold more ADPR-Axin protein in the midgut. Western blot quantification of two independent experimental replicates; ADPR-Axin levels were normalized to the control lines. **F-** *Iduna* mutant clones have elevated GFP-Axin compared to their WT neighbours. A UAS-GFP-Axin transgene was expressed under the temperature sensitive *Myo1A-Gal4* driver in the FRT80B-*Iduna*^{17} mutant. Midgut mutant clones were induced during larval development by daily incubation at 37°C for 1h. Adult female FRT80B-Nls-Red/FRT80B-*Iduna*^{17} flies were collected

after eclosion, incubated at 29°C and analyzed on day 7. Unlabelled cells represent *Iduna*-Null clones, whereas stained for nuclear RFP are either wild type or +/- *Iduna* heterozygous. *p<0.001* is indicated as *** and *p<0.0001* was marked as ****.

Figure 5: A 50% reduction of *Axin* restores ISCs numbers in the *Drosophila* midgut. A- Reducing the *Axin* gene dosage by half restores the number of Arm^{+}/Pros^{-} ISCs. *Axin* mutants *AxinS044230* and *AxnE77* were recombined with the *Iduna^{17}* mutant allele. *AxinS044230* is a complete *Axin*-Null mutant, and *AxinE77* is a loss-of-function truncation allele (Q406X). Midguts of 7d-old adult females of the indicated genotypes were dissected and analyzed by confocal microscopy following Armadillo, Prospero and DAPI staining. *Axin$^{+/-}$:Iduna$^{17/+}$* served as control. Reducing the Axin gene dosage by 50% in *Iduna$^{17/17}$* mutants decreased the number of ISCs to normal levels. **B-** Quantification of ISC numbers. Reducing the *Axin* gene dosage by half fully suppressed the increased numbers of Arm^{+}/Pros^{-} ISCs in *Iduna$^{17/17}$* Null-mutants. **C-** Reducing *Axin* gene expression suppressed the proliferation of ISCs in the *Iduna$^{17/17}$* Null-mutant. *p<0.0001* was marked as ****.

Figure 6: *Iduna* depletion in ECs leads to over-proliferation of ISC. A- Over-proliferation of ISCs in *Iduna* mutants is non-cell autonomous. RNAi-mediated *Iduna* knock-down was carried out in the enterocytes, stem cells and enteroblast cells using *Myo1A-Gal4* and *esg-Gal4* drivers, respectively. **B-** Knock-down of *Iduna* in enterocytes using the *Myo1A-Gal4* driver led to over-proliferation of Arm^{+}/Pros^{-} ISCs. In contrast, no changes in ISC proliferation were observed

upon down-regulation of *Iduna* in ISCs using *esg-Gal4*-driven *Iduna* RNAi. *Myo1A-Gal4*>GFP served as a control. **C-** EC-specific knock-down of *Iduna* increased the number of $pH3^+$ progenitors. **D-** Ectopic expression of *Iduna* in ECs inhibits over-proliferation of ISCs. A UAS-Myc-tagged Iduna C/G transgene was generated to perform rescue experiments. **E- F-** Expression of the UAS-Myc-Iduna C/G transgene with the *Myo1A-Gal4* driver resulted in a reduction of the numbers of $Arm^+/Pros^-$ ISCs and $pH3^+$ mitotic stem cells in the midgut of *Iduna* mutants. 7-day old female midguts were analyzed for ISC and mitotic markers. *p<0.0001* was marked as ****.

Figure 7: Loss of *Iduna* activates the JAK-STAT pathway non-cell autonomously to promote ISC proliferation. A- *Iduna* mutant clones have elevated STAT-GFP signaling in ISCs. *10X-STAT-GFP* is a reporter for STAT pathway activity. *Iduna* mutant clones displayed strongly increased staining of this reporter. **B**- Quantification of STAT-GFP reporter expression in *Iduna* mutant clones. GFP intensity was measured with Image J and normalized with control cells. Iduna mutant clones showed 4-5 fold higher reporter expression. **C-** Knock-down of the *stat93E* transcription factor in ISCs and EBs blocks ISC over-proliferation in *Iduna* mutants. In contrast, RNAi-mediated depletion of *stat92E* in ECs did not affect proliferation of ISCs. **D-** *Iduna* depletion results in upregulation of *Upd3*. *Iduna* was knocked-down using RNAi driven by *Upd3-Gal4*, and *Upd3>GFP* was used as a reporter for *Upd3* gene expression. *White RNAi* served as control. 3-day old female flies were dissected and their posterior midguts were analyzed by confocal microscopy. **E-** Reduction of either *Upd2,*

Upd3 or their receptor *Domeless* suppresses over-proliferation of ISCs in *Iduna* mutants. Upon reduction of *Upd2* and *Upd3* gene dosage by 50%, we observed significantly less mitotic stem cells in *Iduna* mutants, comparable to WT levels. Likewise, a 50% reduction of *Domeless* resulted in suppression of ISC over-proliferation in *Iduna* mutants. On the other hand, these reductions in gene dosage of *Upd2, Upd3* and *Dome* did not affect mitosis of ISCs in a WT background. 7-day old female midguts were quantified by $pH3^+$ staining. n>12 from each genotype. *p<0.0001* was marked as ****. F- Model for the role of *Iduna* in the regulation of intestinal stem cell proliferation. Our model suggests that inactivation of *Iduna* causes Axin elevation which in turn decreases Wingless signaling activation in enterocytes, and increases secretion of UPD cytokines from these cells. These cytokines activate JAK-STAT signaling through the Dome receptor on neighboring ISCs and thereby induce ISC proliferation in the *Drosophila* midgut.

Supplementary Figure Legends

Figure S1: Intestinal stem cells in the *Drosophila* midgut give rise to enterocytes and enteroendocrine cells. A- ISCs give rise to two different types of daughter progenitors, undifferentiated enteroblasts (EBs) and pre-enteroendocrine cells (Pre-EE). EBs and pre-EEs differentiate into enterocytes (ECs) and enteroendocrine (EEs) cells, respectively. **B-** ISCs and ECs can be distinguished by their cell sizes, high level of membrane-associated Armodillo, and lack of nuclear Prospero. On the other hand, differentiated EEs are small and can be identified by nuclear Prospero staining. Finally, small-sized ISCs are stained with Armodillo but not with nuclear Prospero. In the image, small ISCs were co-stained with escargot (green), and Armodillo (red). On the other hand, small EEs were shown with the red arrow and stained with Armadillo (red) and nuclear Prospero (red). Bigger cells are enterocytes whose cell membrane is stained with Armodillo (red). DAPI staining in blue marks the cell nucleus.

Figure S2: Iduna is not required for differentiation of ISC. A- *Iduna* mutants contain slightly more cells in their midgut. It appears that an increase in ISC number is responsible for this effect. **B-D-** No differences in the numbers of enterocytes and enteroendocrine cells were observed in *Iduna* mutants. **E-H-** Iduna is not required for the differentiation of ISCs into enterocytes. Enterocytes were marked with GFP expressed under the control of enterocyte specific driver, *Myo1A-Gal4*. 7-day old mutant clones were analyzed. Control cells are shown with nuclear RFP, and *Iduna* mutant clones are marked with a white line. **G-M-** Genetic depletion of *Iduna* did not affect the differentiation of ISCs into

enteroendocrine cells. Mutant clones in 7d-old adult midguts were analyzed with Prospero staining. Small nuclear Prospero-positive EE cells are labelled with yellow arrows in *Iduna* mutant clones. Control cells are labelled with nuclear RFP, and mutant clones are marked with a white line.

Material and Methods

Fly stocks: Flies were kept at a 12-hour light/dark cycle. All crosses were performed at 22-25°C, unless stated otherwise. The following fly stocks were used for this study (Bloomington Drosophila Stock Center (BDSC) and Vienna Drosophila Resource Center (VDRC) number (#) given in parentheses):

The stocks used in here: Df(3L)Exel6135 (BDSC# 7614), Df(3L)ED228 (BDSC# 8086), Df(3L)ED229 (BDSC# 8087), esg-Gal4, UAS-GFP (a gift of Dr. Norbert Perrimon, Micchelli et al., 2006), esgK606 (a gift of Dr. Norbert Perrimon, Micchelli et al., 2006), *10X STAT-GFP*, Bach et al., 2007), UAS-GFP-Axin (BDSC# 7224), FRT82B, *Axin044230* (a gift of Dr. Wei Du, Hamada et al., 1999), FRT82B, *AxinE77* (a gift of Dr. Jessica Treisman, Collins et al., 2000), BAC Axin-V5 (a gift of Dr. Jean-Paul Vincent, Gerland et al., 2014), Myo1A-Gal4, tub-Gal80ts, UAS-GFP (a gift of Dr. Norbert Perrimon, Micchelli et al., 2006), Upd3-Gal4, UAS-GFP (a gift of Dr. Norbert Perrimon, Markstein et al., 2013), ΔUpd2/3 (BDSC# 129), ΔDome (BDSC# 12030), UAS-*stat92E* RNAi (BDSC# 26889), UAS-CG8786/*dIduna* RNAi#1 (BDSC# 40882), UAS-CG8786/*dIduna* RNAi#2 (VDRC#43533), UAS-CG8786/*dIduna* RNAi#3 (VDRC#36028), UAS-CG8786/*dIduna* RNAi#4 (VDRC#36029), and White RNAi (BDSC#33623). The rest of *Drosophila* lines, which were studied in here, were obtained from Steller Lab stocks. Oregon R flies were used as control and only adult female flies were analyzed in this study.

***CG8786/dRNF146/dIduna* CRISPR/Cas9 editing:** We used the CRISPR optimal target finder website (tools.flycrispr.molbio.wisc.edu/targetFinder) to identify an

appropriate guide RNA (gRNA) target sequence within *dIduna* (Granz et al., 2013 and 2014). We purchased the forward 5`-GTCGCTAGCTGCAATCTGCTCTG-3` and reverse 5`-AAACCAGAGCAGATTGCAGCTAG-3` oligos (IDT, Inc.) annealed, and followed the protocol; from Port et al., 2014 to clone the annealed oligos into pCFD3-dU6:3gRNA plasmid (Addgene, plasmid# 49410, Port et al., 2014). Transformants were verified via Sanger sequencing (Genewiz, Inc.). The gRNA plasmid was injected into 300 embryos of custom *vasa*-Cas9 *Drosophila* (BestGene, Inc.). The injection was yielded 89 G_o progeny, and we established 70 individual fly lines, a couple of which could possibly have the Iduna loss-of-function mutations.

Isolation of the *Iduna* mutants and genetic mapping of *Iduna* –loss-of-function mutations: Total DNA was isolated from L3 larvae or 5-days old adults of *Iduna* homozygous mutants and control sequencing strain using the Roche genomic DNA extraction kit (Roche). To confirm the mutant line, PCR fragments were amplified with specific primers (forward primer 5`-CAGCCCGAGCTGGTCATACTCAG-3`, reverse primer 5`-CGGCTTTCTGGGCTACCTAC-3`) binding within 5` UTR of *Iduna* and within the coding region of the gene. To identify mutation site, the entire coding region was PCR amplified and PCR products were sent for DNA sequencing.

Cloning and generation of UAS-CG8786 transgenic *Drosophila*: Adult flies were directly homogenized in 1 ml TRIzol (Life Technologies) and total RNA was isolated according to the manufacturer's protocol. cDNA library was prepared from 5 µg total RNA, by using oligo(dT) amplification and the Superscript III First

Strand synthesis kit (Invitrogen). cDNA library was used to amplify the *Iduna* transcripts with the primers (forward 5`-ATGTCGCAACAGCGCTCCACAG-3`; *Iduna* B isoform reverse primer 5`-TCAGTAGAGCTTTAGGTATACC-3`; *Iduna* C/G isoform reverse primer 5`-TCAGTAGAGCTTTAGGTATACCG-3`). Amplified *dIduna* transcripts were cloned into pUAST (DGRC, Drosophila Genomic Resource Center) and pAc5.1 (Thermo Scientific) vectors by considering the appropriate restriction digestion sites. Following the bacterial transformation, all of the cloned genes were sequenced. To generate UAS-CG8786 transgenic *Drosophila,* myc-tagged pUAST-CG8786/dIduna plasmid was injected into w1118 embryos (Best Gene, Inc.) We obtained successful transgenic lines.

Cloning and generation of the wild type and mutants UAS-Flag-Tnks transgenic *Drosophila*: We previously described *Drosophila* TNKS (Park and Steller, 2013) and its ORF was cloned into pUAST vector from pcDNA3.1-Flag-TNKS. To generate UAS-Flag-TNKS transgenic *Drosophila,* Flag-tagged pUAST-TNKS plasmid was injected into w1118 embryos (Best Gene, Inc.) We obtained successful transgenic *Drosophila* lines and those were utilized in conjunction with tissue-specific *Gal4* drivers.

Clone analysis and RNAi experiments: Mutant clones were utilized to generate mitotic clones. 2nd instar larvae were subjected to an hour heat shock in a 37^{0}C water bath per day until they reached the pupa stage and maintained at 24^{0}C. 3-days old adult females were analyzed.

For RNAi experiment, crosses were performed at 24^{0}C and the progeny of the desired genotypes were collected on the day of enclosion and maintained at

24^0C for 7 days before dissection. In the case of using temperature sensitive driver, enclosed virgin females were collected and kept at 29^0C for 7 days for intestine dissection.

Cell culture: S2R+ cells were maintained at 25°C in supplemented Grace's Insect Medium (supplemented with 10% heat inactivated FBS, 100 U/ml penicillin, 100 µg/ml streptomycin) in spinner flasks.

Development of polyclonal antibodies: Full-length GST-tagged-Iduna C/G protein was expressed and purified from BL21 DE3 *E.coli* strain. Polyclonal antisera were generated in two guinea pigs (Cocalico, Inc.). For Western blot analysis, serum was used in 1:1000 dilutions.

Western blot analysis: 50-100µg dissected tissues or total larvae/flies were lysed in lysis buffer [50mM HEPES-KOH pH 7.4, 150mM NaCl, 0.05% Triton-X100, complete EDTA-free protease inhibitor cocktail (Roche)] using a 1 ml tissue grinder. Lysates were cleared by centrifugation at 13,000 g for 20 min at 4°C. Protein concentrations of supernatants were determined by BCA assay (Pierce). 1µg/ul lysate was prepared with 3X sample buffer in 100ul total volume (200mM Tris-HCl, pH 6.8, 200mM dithiothreitol (DTT), 8% SDS, 24% glycerol, 0.04% bromophenol blue), heated at 95°C for 10 min and samples were separated by SDS-PAGE for 1 h at 120V, by using standard 1X SDS Tris base-glycine running buffer. Proteins on the gels were blotted onto a PVDF membrane, in a 1X transfer buffer (25mM Tris base, 190mM Glycine, 20% MeOH, 0.05% SDS), and transferred (Bio-Rad) at 100V for 90 min. Membranes were taken through a standard immunoblot protocol followed by enhanced

chemiluminescent detection (Crescendo ECL, Millipore) using a Lumimager (Fuji, LAS-3000). Primary antibodies: α- tubulin (1/1000, Sigma), α-flag (1/1000, Cell Signaling Technologies), α-myc tag (1/1000, Cell Signaling Technologies) (GFP (1/2500, Santa Cruz), β-actin (1/1000), anti-PAR (1/1000, Trevigen). Secondary antibodies: anti mouse, anti rabbit, anti guinea pig (1/5000, Jackson Labs).

Immunofluorescence: Adult intestines were dissected in 1xPBS and fixed in 4% paraformaldehyde in PBS for 45 min at room temperature. Tissues then, were first washed with 0.1% Tween 20-PBS, second washed with 0.1% TritonX-100-PBS and finally permeabilized in 0.5% TritonX 100-PBS for 30 min. Following the blocking with 10% BSA in 0.1% Tween 20-PBS for 1h at room temperature, primary antibody incubation in 10% BSA in 0.1% Tween 20-PBS was performed for overnight at 4°C. 3X 5 min 0.1% Tween 20-PBS washed intestines then were incubated in secondary antibodies for 1h at room temperature. Specimens were finally mounted in Fluoromount-G (Southern Biotech) and analyzed with confocal imaging. Primary antibodies: mouse anti-Arm (N2 7A1, DSHB, 1:50), mouse anti-Prospero (MR1A, DSHB, 1/50), mouse anti-GFP (GFP-12A6, DSHB, 1/100), mouse anti-β-galactosidase (40-1a, DSHB, 1/100), mouse anti-Delta (C594.9B, DSHB, 1/100), rabbit anti-phosho-S10-Histone3 (06-570, Millipore, 1/1000). The secondary antibodies were Alexa fluorophores (Thermo Fisher Scientific) and diluted as 1/1000.

Immunoprecipitation: S2R+ cells were seeded at $5x10^6$ cells/10 cm^2 culture plates and incubated overnight at 25^0C. Cells were then co-transfected with 5μg of each plasmid by using Mirus-insect transfection reagent. Negative control was

transfected with empty plasmids. 48 hours later, transfected cells were harvested. The cell pellets were washed within cold 1X PBS. This step was repeated 3 times. Pellets were re-suspended in 600µl 1% Triton X-100 lysing buffer. Re-suspended pellets were incubated on ice for 15 min and mixed gently and periodically. Total lysates were centrifuged at 13,000 rpm at 4^0C for 30 minutes. The supernatant was removed and 100µl was stored as total lysate. 25µl Protein A/G (Thermo Scientific) beats were washed with lysing buffer for 3 times. 200µl supernatant was incubated with the mixture of washed protein A-G beads on the rotator at cold room for 30 minutes. In a parallel way, 25µl Protein A /G was washed with lysing buffer for 3 times. At the end of incubation period, beads-supernatant mixture was centrifuged at 2,000 rpm at 4^0C for 1 minute. Pre-cleaned supernatant was collected and added to beads. Antibody was added to supernatant-beads and incubated at cold room on rotator for 4 h. Beads-supernatant-antibody mixture was centrifuged at 2,000 rpm at 4^0C for 1 minute and beads were washed with lysing buffer for 3 times. In the final step, beads were re-suspended in 50µl of 3X sample buffer to perform immunoblotting.

Recombinant protein purification from S2R+ cells: S2R+ cells were seeded at $5x10^6$ cells/10 cm^2 culture plates and incubated overnight at 25^0C. Then, flag or myc-tagged gene of interests were transfected and based on the small tag, a recombinant protein was immunoprecipitated with flag or myc agarose beads as described above. Finally, by using flag or myc peptides, tagged proteins were eluted and quantified by BCA (Pierce, ThermoFisher Scientific).

Quantification and statistics: ISC quantification, dissected midguts were stained with Armodillo and Prospero. Images of the R5a region (Buchon et al., 2013) were obtained with a 63X objective and total number of $Arm^{+}/Pros^{-}$ cells in a field were counted. Quantifications of immunoblot were done with Image J. Student *t-test* and ANOVA were used as statistical analysis and those were done with Prism (GraphPad) software.

Author Contributions: HS and YG designed the concept of the study. YG performed all experiments. YG and HS jointly wrote the manuscript.

Acknowledgments: We would like to thank all members of the Steller Lab for their helpful suggestions and discussions, especially Adi Minis and Junko Shimazu for critical reading of the ms. We also thank Drs. Norbert Perrimon, Jean-Paul Vincent, Wei Du, Jessica Treisman, and Steven X. Hou for sharing their published *Drosophila* lines, the Bloomington Stock Center and the Vienna *Drosophila* Research Center for the fly stocks, and the *Drosophila* Genomics Resource Center and Developmental Studies Hybridroma Bank for reagents. This work was supported by NIH grant RO1GM60124 to H.S.

The authors declare no competing interests.

References

Andreu P., Colnot, S., Godard, C., Gad, S., Chafey, P., Niwa-Kawakita, M., Laurent-Puig, P., Kahn, A., Robine, S., Perret, C., Romagnolo, B. (2005). Crypt-restricted proliferation and commitment to the Paneth cell lineage following Apc loss in the mouse intestine. Development. 132(6):1443-51.

Bach, E.A., Ekas, L.A., Ayala-Camargo, A., Flaherty, M.S., Lee, H., Perrimon, N., and Baeg, G.H. (2007). GFP reporters detect the activation of the *Drosophila* JAK/STAT pathway in vivo. Gene Expr. Patterns *7*, 323–331.

Buchon, N., Osman, D., David, F.P.A., Yu Fang, H., Boquete, J.P., Deplancke, B., and Lemaitre, B. (2013). Morphological and Molecular Characterization of Adult Midgut Compartmentalization in *Drosophila*. Cell Rep. *3*, 1725–1738.

Callow, M.G., Tran, H., Phu, L., Lau, T., Lee, J., Sandoval, W.N., Liu, P.S., Bheddah, S., Tao, J., Lill, J.R., et al. (2011). Ubiquitin ligase RNF146 regulates Tankyrase and Axin to promote Wnt signaling. PLoS One 6(7): e22595

Chiang, Y.J., Hsiao, S.J., Yver, D., Cushman, S.W., Tessarollo, L., Smith, S., and Hodes, R.J. (2008). Tankyrase 1 and Tankyrase 2 are essential but redundant for mouse embryonic development. PLoS One *3*, e2639.

Cho-Park, P.F., and Steller, H. (2013). Proteasome regulation by ADP-ribosylation. Cell *153*, 614–627.

Clevers, H., and Nusse, R. (2012). Wnt/β-catenin signaling and disease. Cell *149*, 1192–1205.

Collins, R.T., and Treisman, J.E. (2000). Osa-containing Brahma chromatin remodeling complexes are required for the repression of Wingless target genes. Genes Dev. *14*, 3140–3152.

Cordero, J.B., Stefanatos, R.K., Scopelliti, A., Vidal, M., and Sansom, O.J. (2012). Inducible progenitor-derived Wingless regulates adult midgut regeneration in *Drosophila*. EMBO J. *31*, 3901–3917.

Croy, H.E., Fuller, C.N., Giannotti, J., Robinson, P., Foley, A.V.A., Yamulla, R.J., Cosgriff, S., Greaves, B.D., Von Kleeck, R.A., An, H.H., et al. (2016). The poly(ADP-ribose) polymerase enzyme Tankyrase antagonizes activity of the β-catenin destruction complex through ADP-ribosylation of Axin and APC2. J. Biol. Chem. *291*, 12747–12760.

DaRosa, P.A., Wang, Z., Jiang, X., Pruneda, J.N., Cong, F., Klevit, R.E., and Xu, W. (2014). Allosteric activation of the RNF146 ubiquitin ligase by a polyADP-ribosylation signal. Nature. *8*; 517(7533): 223.

Feng, Y., Li, X., Ray, L., Song, H., Qu, J., Lin, S., and Lin, X. (2014). The *Drosophila* Tankyrase regulates Wg signaling depending on the concentration of dAxin. Cell. Signal. *26*, 1717–1724.

Fevr, T., Robine, S., Louvard, D., and Huelsken, J. (2007). Wnt/ β-catenin is essential for intestinal homeostasis and maintenance of intestinal stem cells. Mol. Cell. Biol. *27*, 7551–7559.

Gerlach, J.P., Emmink, B.L., Nojima, H., Kranenburg, O., and Maurice, M.M. (2014). Wnt signalling induces accumulation of phosphorylated β-catenin in two distinct cytosolic complexes. Open Biol. *4*, 140120–140120.

Ghiglione, C., Devergne, O., Georgenthum, E., Carballès, F., Médioni, C., Cerezo, D., Noselli, S. (2002). The *Drosophila* cytokine receptor Domeless controls border cell migration and epithelial polarization during oogenesis. Development *129*, 5437–5447.

Gratz, S.J., Cummings, A.M., Nguyen, J.N., Hamm, D.C., Donohue, L.K., Harrison, M.M., Wildonger, J., and O'connor-Giles, K.M. (2013). Genome engineering of *Drosophila* with the CRISPR RNA-guided Cas9 nuclease. Genetics *194*, 1029–1035.

Gratz, S.J., Ukken, F.P., Rubinstein, C.D., Thiede, G., Donohue, L.K., Cummings, A.M., and Oconnor-Giles, K.M. (2014). Highly specific and efficient CRISPR/Cas9-catalyzed homology-directed repair in *Drosophila*. Genetics *196*, 961–971.

Hamada, F., Tomoyasu, Y., Takatsu, Y., Nakamura, M., Nagai, S.I., Suzuki, A., Fujita, F., Shibuya, H., Toyoshima, K., Ueno, N., et al. (1999). Negative regulation of Wingless signaling by D-Axin, a Drosophila homolog of Axin. Science. *283*, 1739–1742.

Hsiao, S.J., Poitras, M.F., Cook, B.D., Liu, Y., and Smith, S. (2006). Tankyrase 2 Poly(ADP-Ribose) polymerase domain-deleted mice exhibit growth defects but have normal telomere length and capping. Mol. Cell. Biol. *26*, 2044–2054.

Huang, S.M.A., Mishina, Y.M., Liu, S., Cheung, A., Stegmeier, F., Michaud, G.A., Charlat, O., Wiellette, E., Zhang, Y., Wiessner, S., et al. (2009). Tankyrase inhibition stabilizes Axin and antagonizes Wnt signalling. Nature *461*, 614–620.

Kinzler, K., Nilbert, M., Su, L., Vogelstein, B., Bryan, T., Levy, D., Smith, K., Preisinger, A., Hedge, P., McKechnie, D., et al. (1991). Identification of FAP locus genes from chromosome 5q21. Science. *253*, 661–665.

Korinek, V., Barker, N., Morin, P.J., van Wichen, D., de Weger, R., Kinzler, K.W., Vogelstein, B., and Clevers, H. (1997). Constitutive transcriptional activation by a beta-catenin-Tcf complex in $APC^{-/-}$ colon carcinoma. Science *275*, 1784–1787.

Korinek, V., Barker, N., Moerer, P., Van Donselaar, E., Huls, G., Peters, P.J., and Clevers, H. (1998). Depletion of epithelial stem-cell compartments in the small intestine of mice lacking Tcf-4. Nat. Genet. *19*, 379–383.

Kramps, T., Peter, O., Brunner, E., Nellen, D., Froesch, B., Chatterjee, S., Murone, M., Züllig, S., and Basler, K. (2002). Wnt/Wingless signaling requires BCL9/legless-mediated recruitment of pygopus to the nuclear β-catenin-TCF complex. Cell *109*, 47–60.

Lee, E., Salic, A., Krüger, R., Heinrich, R., and Kirschner, M.W. (2003). The roles of APC and Axin derived from experimental and theoretical analysis of the Wnt pathway. PLoS Biol. *1*.

Li, V.S.W., Ng, S.S., Boersema, P.J., Low, T.Y., Karthaus, W.R., Gerlach, J.P., Mohammed, S., Heck, A.J.R., Maurice, M.M., Mahmoudi, T., et al. (2012). Wnt signaling through inhibition of β-catenin degradation in an intact Axin1 Complex. Cell *149*, 1245–1256.

Lin, G., Xu, N., and Xi, R. (2008). Paracrine Wingless signalling controls self-renewal of *Drosophila* intestinal stem cells. Nature *455*, 1119–1123.

Lu, J., Ma, Z., Hsieh, J.C., Fan, C.W., Chen, B., Longgood, J.C., Williams, N.S., Amatruda, J.F., Lum, L., and Chen, C. (2009). Structure-activity relationship studies of small-molecule inhibitors of Wnt response. Bioorganic Med. Chem. Lett. *19*, 3825–3827.

Markstein, M., Dettorre, S., Cho, J., Neumuller, R.A., Craig-Muller, S., and Perrimon, N. (2014). Systematic screen of chemotherapeutics in *Drosophila* stem cell tumors. Proc. Natl. Acad. Sci. *111*, 4530–4535.

Matsumoto, Y., La Rose, J., Lim, M., Adissu, H.A., Law, N., Mao, X., Cong, F., Mera, P., Karsenty, G., Goltzman, D., et al. (2017). Ubiquitin ligase RNF146 coordinates bone dynamics and energy metabolism. J. Clin. Invest. *127*, 2612–2625.

Matsumoto, Y., Larose, J., Kent, O.A., Lim, M., Changoor, A., Zhang, L., Storozhuk, Y., Mao, X., Grynpas, M.D., Cong, F., et al. (2017). RANKL coordinates multiple osteoclastogenic pathways by regulating expression of ubiquitin ligase RNF146. J. Clin. Invest. *127*, 1303–1315.

Micchelli, C.A., and Perrimon, N. (2006). Evidence that stem cells reside in the adult *Drosophila* midgut epithelium. Nature *439*, 475–479.

Morin, P.J., Sparks, a B., Korinek, V., Barker, N., Clevers, H., Vogelstein, B., and Kinzler, K.W. (1997). Activation of beta-catenin-Tcf signaling in colon cancer by mutations in beta-catenin or APC. Science *275*, 1787–1790.

Nishisho, I., Nakamura, Y., Miyoshi, Y., Miki, Y., Ando, H., Horii, A., Koyama, K., Utsunomiya, J., Baba, S., and Hedge, P. (1991). Mutations of chromosome 5q21 genes in FAP and colorectal cancer patients. Science. *253*, 665–669.

Nusse, R., and Clevers, H. (2017). Wnt/β-catenin signaling, disease, and emerging therapeutic modalities. Cell *169*, 985–999.

Ohlstein, B., and Spradling, A. (2006). The adult *Drosophila* posterior midgut is maintained by pluripotent stem cells. Nature *439*, 470–474.

Port, F., Chen, H.-M., Lee, T., and Bullock, S.L. (2014). Optimized CRISPR/Cas tools for efficient germline and somatic genome engineering in *Drosophila*. Proc. Natl. Acad. Sci. *111*, E2967–E2976.

Rubinfeld, B., Robbins, P., El-Gamil, M., Albert, I., Porfiri, E., and Polakis, P. (1997). Stabilization of beta-catenin by genetic defects in melanoma cell lines. Science *275*, 1790–1792.

Saito-Diaz, K., Benchabane, H., Tiwari, A., Tian, A., Li, B., Thompson, J.J., Hyde, A.S., Sawyer, L.M., Jodoin, J.N., Santos, E., et al. (2018). APC inhibits ligand-independent Wnt signaling by the clathrin endocytic pathway. Dev. Cell *44*, 566–581.e8.

Salic, A., Lee, E., Mayer, L., and Kirschner, M.W. (2000). Control of β-catenin stability: Reconstitution of the cytoplasmic steps of the Wnt pathway in *Xenopus* egg extracts. Mol. Cell *5*, 523–532.

Theodosiou, N.A., and Xu, T. (1998). Use of FLP/FRT system to study *Drosophila* development. Methods A Companion to Methods Enzymol. *14*, 355–365.

Tian, A., Benchabane, H., Wang, Z., and Ahmed, Y. (2016). Regulation of stem cell proliferation and cell fate specification by Wingless/Wnt signaling gradients enriched at adult intestinal compartment boundaries. PLoS Genet. *12*.

Wang, Z., Tian, A., Benchabane, H., Tacchelly-Benites, O., Yang, E., Nojima, H., and Ahmed, Y. (2016a). The ADP-ribose polymerase Tankyrase regulates adult intestinal stem cell proliferation during homeostasis in *Drosophila*. Development *143*, 1710–1720.

Wang, Z., Tacchelly-Benites, O., Yang, E., Thorne, C.A., Nojima, H., Lee, E., and Ahmed, Y. (2016b). Wnt/wingless pathway activation is promoted by a critical threshold of axin maintained by the tumor suppressor APC and the ADP-ribose polymerase Tankyrase. Genetics *203*, 269–281.

Xu, N., Wang, S.Q., Tan, D., Gao, Y., Lin, G., and Xi, R. (2011). EGFR, Wingless and JAK/STAT signaling cooperatively maintain *Drosophila* intestinal stem cells. Dev. Biol. *354*, 31–43.

Yang, E., Tacchelly-Benites, O., Wang, Z., Randall, M.P., Tian, A., Benchabane, H., Freemantle, S., Pikielny, C., Tolwinski, N.S., Lee, E., et al. (2016). Wnt pathway activation by ADP-ribosylation. Nat. Commun. *7*.

Zeidler, M.P., Bach, E.A., and Perrimon, N. (2000). The roles of the *Drosophila* JAK/STAT pathway. Oncogene *19*, 2598–2606.

Zhang, Y., Liu, S., Mickanin, C., Feng, Y., Charlat, O., Michaud, G.A., Schirle, M., Shi, X., Hild, M., Bauer, A., et al. (2011). RNF146 is a poly(ADP-ribose)-directed E3 ligase that regulates Axin degradation and Wnt signalling. Nat. Cell Biol. *13*, 623–629.

Zhou, F., Rasmussen, A., Lee, S., and Agaisse, H. (2013). The UPD3 cytokine couples environmental challenge and intestinal stem cell division through modulation of JAK/STAT signaling in the stem cell microenvironment. Dev. Biol. *373*, 383–393.

Zoranovic, T., Grmai, L., and Bach, E. (2013). Regulation of proliferation, cell competition, and cellular growth by the *Drosophila* JAK-STAT pathway. Jak-Stat *2*, e25408.

Figure 1

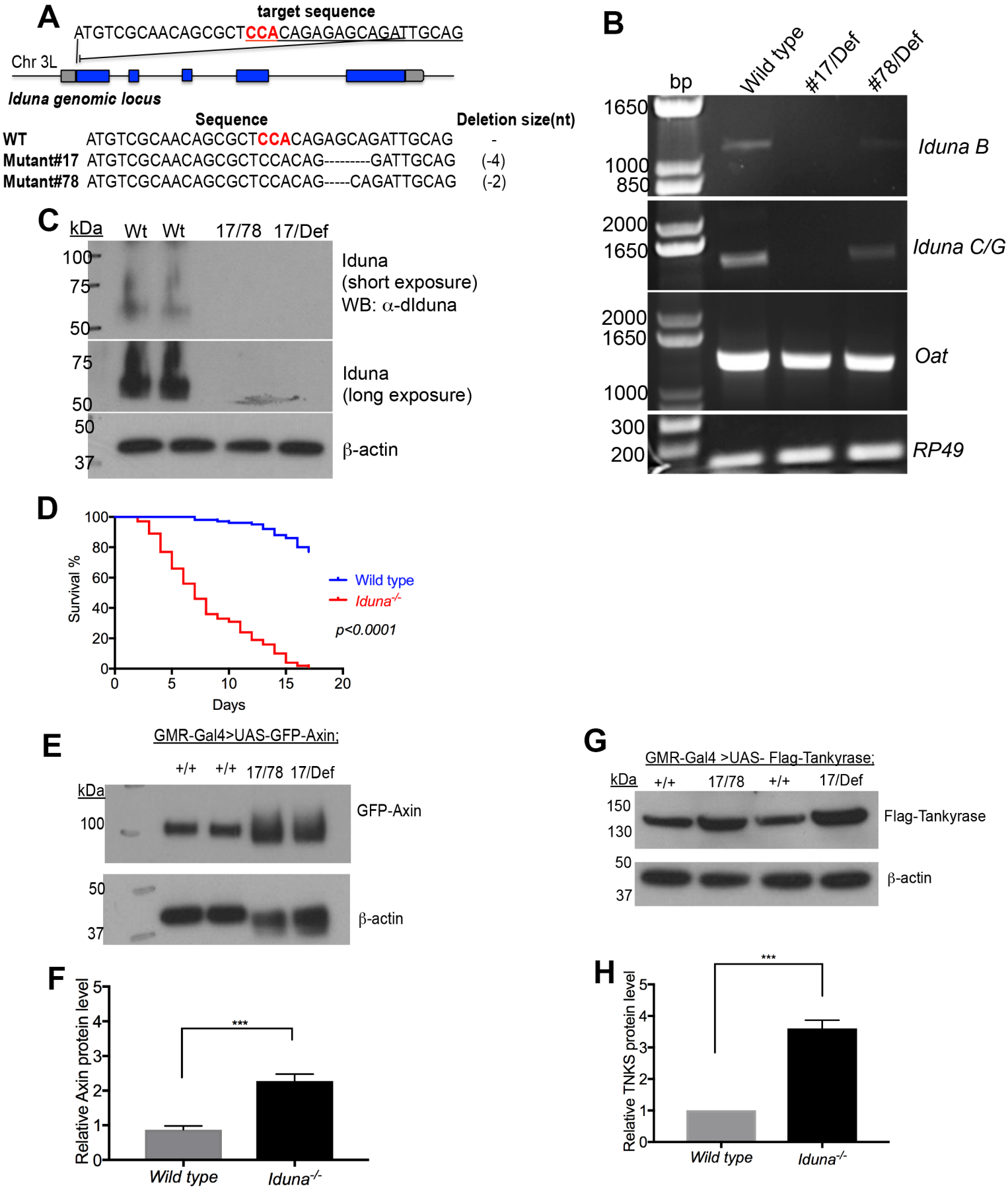
A
target sequence
ATGTCGCAACAGCGCTCCACAGAGAGCAGATTGCAG
Chr 3L
Iduna genomic locus
Sequence
Deletion size(nt)
WT ATGTCGCAACAGCGCTCCACAGAGCAGATTGCAG -
Mutant#17 ATGTCGCAACAGCGCTCCACAG---------GATTGCAG (-4)
Mutant#78 ATGTCGCAACAGCGCTCCACAG-----CAGATTGCAG (-2)
B
bp
Wild type
#17/Def
#78/Def
1650
1000
850
Iduna B
2000
1650
Iduna C/G
2000
1650
1000
Oat
300
200
RP49
C
kDa
Wt Wt 17/78 17/Def
100
75
50
Iduna
(short exposure)
WB: α-dIduna
75
50
Iduna
(long exposure)
50
37
β-actin
D
Survival %
Days
Wild type
Iduna-/-
p<0.0001
E
GMR-Gal4>UAS-GFP-Axin;
+/+ +/+ 17/78 17/Def
kDa
100
GFP-Axin
50
37
β-actin
F
Relative Axin protein level
***
Wild type
Iduna-/-
G
GMR-Gal4 >UAS- Flag-Tankyrase;
kDa
+/+ 17/78 +/+ 17/Def
150
130
Flag-Tankyrase
50
37
β-actin
H
Relative TNKS protein level
***
Wild type
Iduna-/-

Figure 2

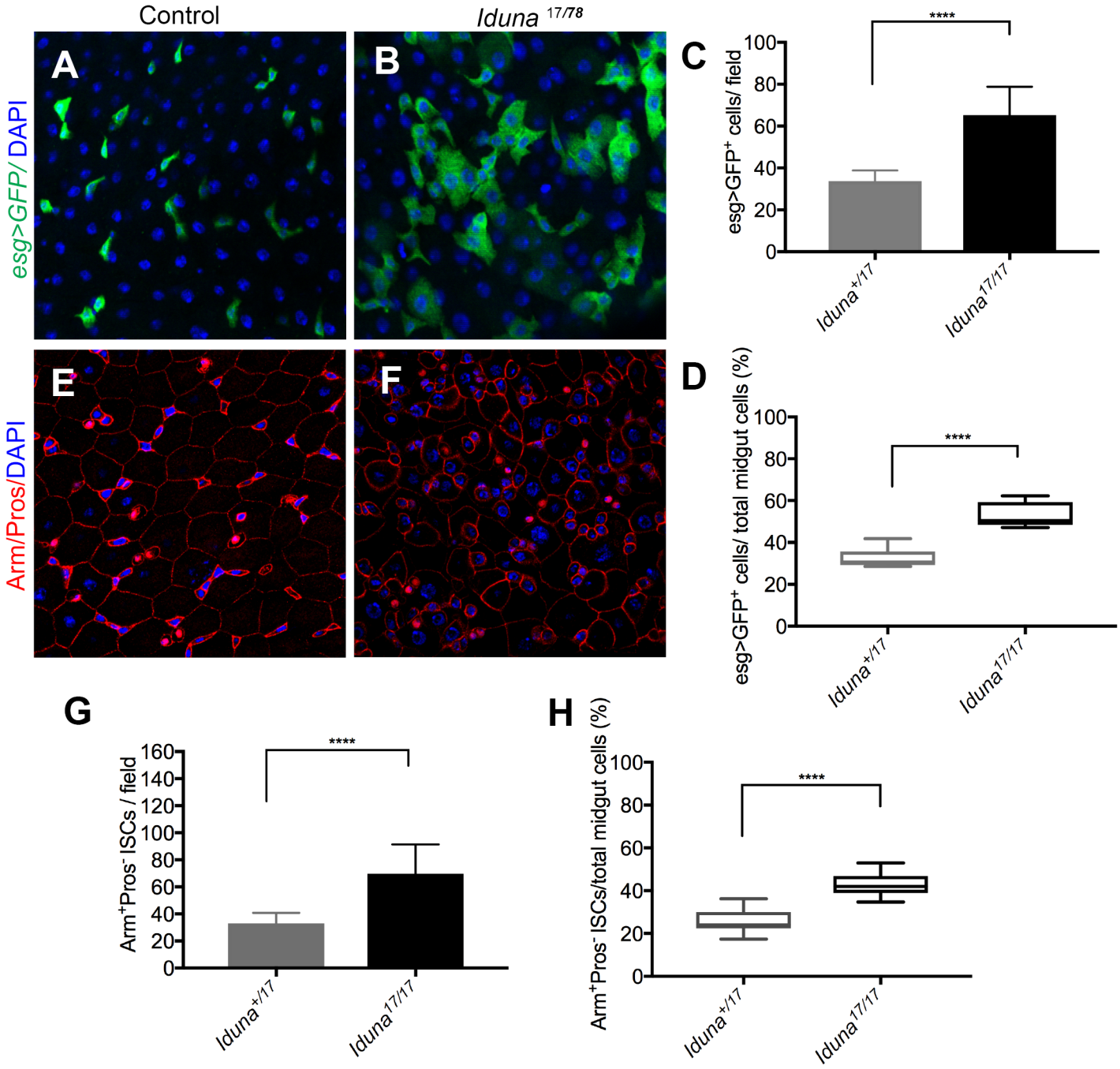
Control
Iduna 17/78
A
B
C
D
E
F
G
H
esg>GFP/ DAPI
Arm/Pros/DAPI
esg>GFP+ cells/ field
esg>GFP+ cells/ total midgut cells (%)
Arm+Pros- ISCs / field
Arm+Pros- ISCs/total midgut cells (%)
****
Iduna+/17
Iduna17/17

Figure 3

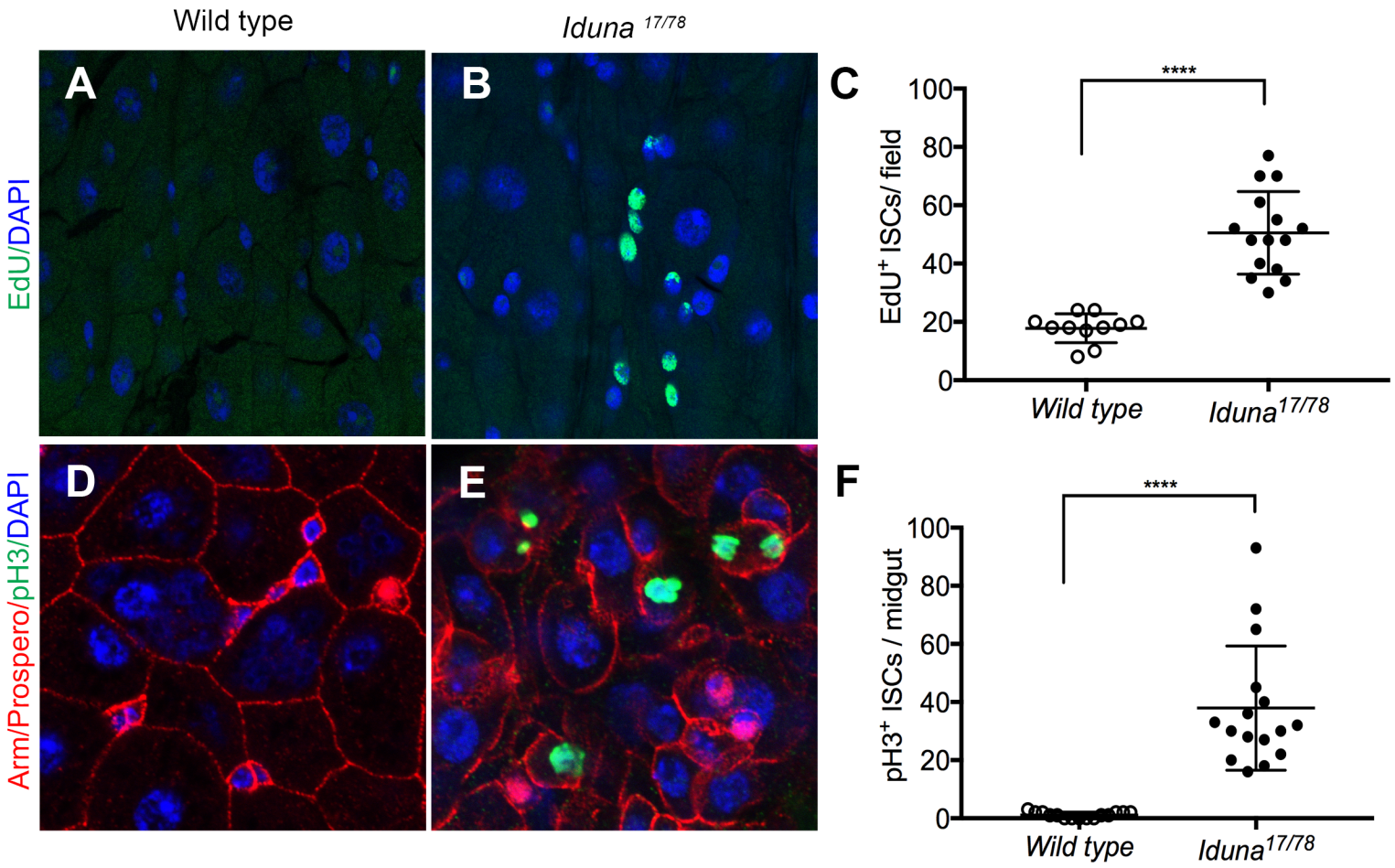
Wild type
Iduna 17/78
A
B
C
D
E
F
EdU/DAPI
Arm/Prospero/pH3/DAPI
EdU+ ISCs/ field
pH3+ ISCs / midgut
****
****
100
80
60
40
20
0
Wild type
Iduna17/78

Figure 4

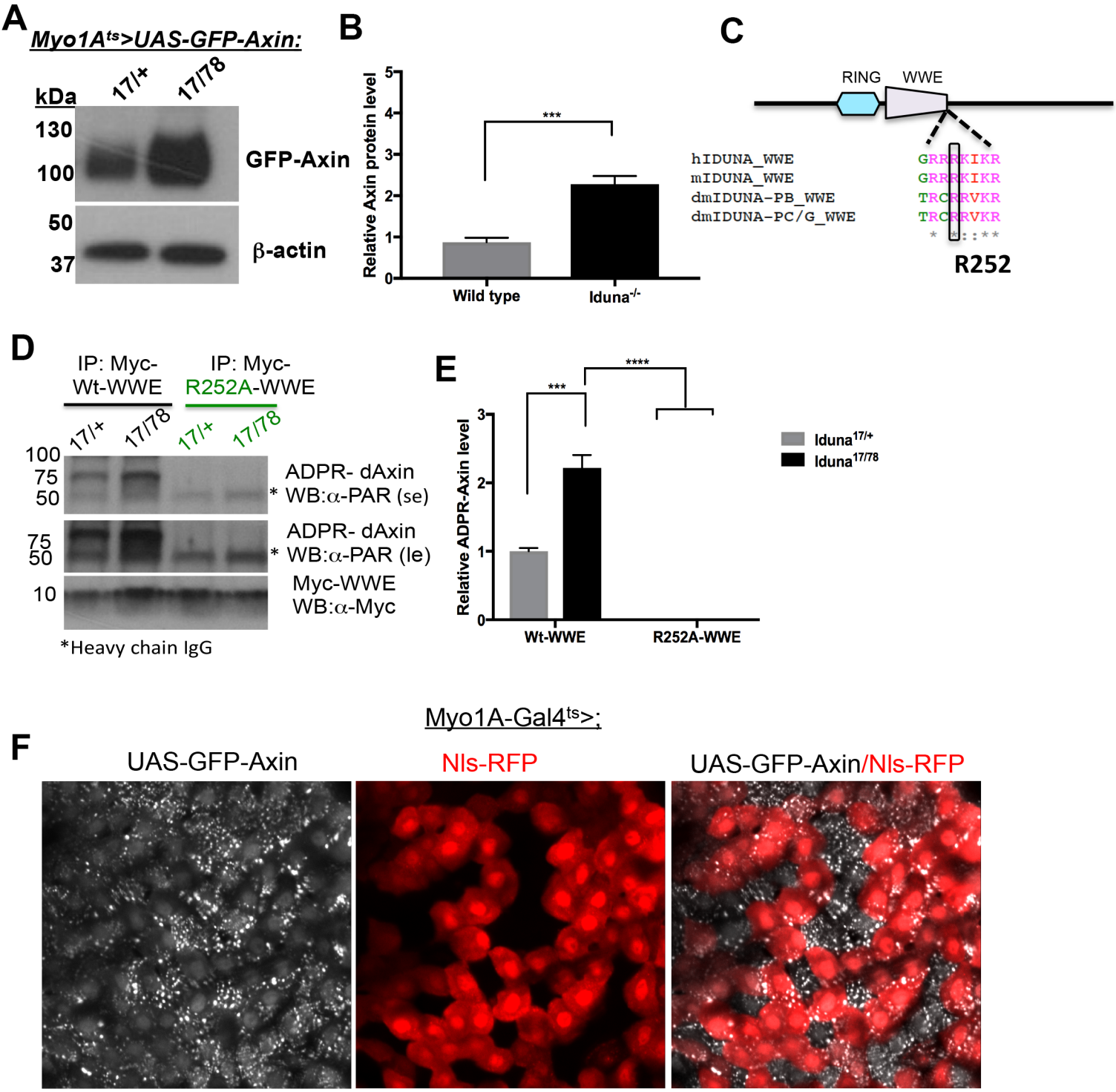
A
Myo1A^ts>UAS-GFP-Axin:
kDa
17/+
17/78
130
100
50
37
GFP-Axin
β-actin
B
Relative Axin protein level
***
Wild type
Iduna-/-
C
RING
WWE
hIDUNA_WWE
mIDUNA_WWE
dmIDUNA-PB_WWE
dmIDUNA-PC/G_WWE
GRRRKIKR
GRRRKIKR
TRCRRVKR
TRCRRVKR
R252
D
IP: Myc-Wt-WWE
IP: Myc-R252A-WWE
17/+
17/78
17/+
17/78
100
75
50
ADPR- dAxin
WB:α-PAR (se)
75
50
ADPR- dAxin
WB:α-PAR (le)
10
Myc-WWE
WB:α-Myc
*Heavy chain IgG
E
Relative ADPR-Axin level
***
****
Wt-WWE
R252A-WWE
Iduna17/+
Iduna17/78
Myo1A-Gal4ts>;
F
UAS-GFP-Axin
Nls-RFP
UAS-GFP-Axin/Nls-RFP

Figure 5

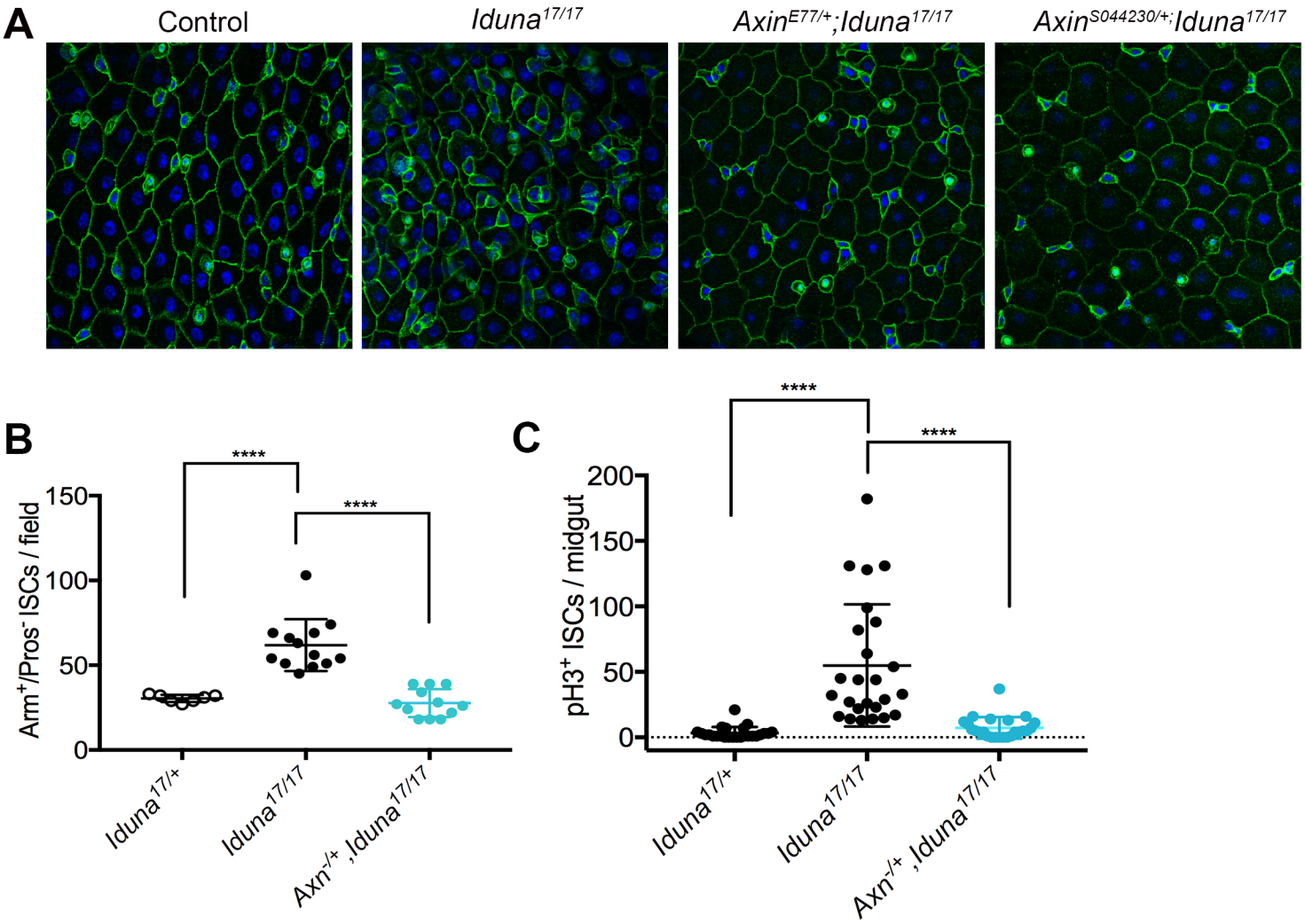
A
Control
Iduna17/17
AxinE77/+;Iduna17/17
AxinS044230/+;Iduna17/17
B
Arm+/Pros- ISCs / field
150
100
50
0
****
****
Iduna17/+
Iduna17/17
Axn-/+ ;Iduna17/17
C
pH3+ ISCs / midgut
200
150
100
50
0
****
****
Iduna17/+
Iduna17/17
Axn-/+ ;Iduna17/17

Figure 6

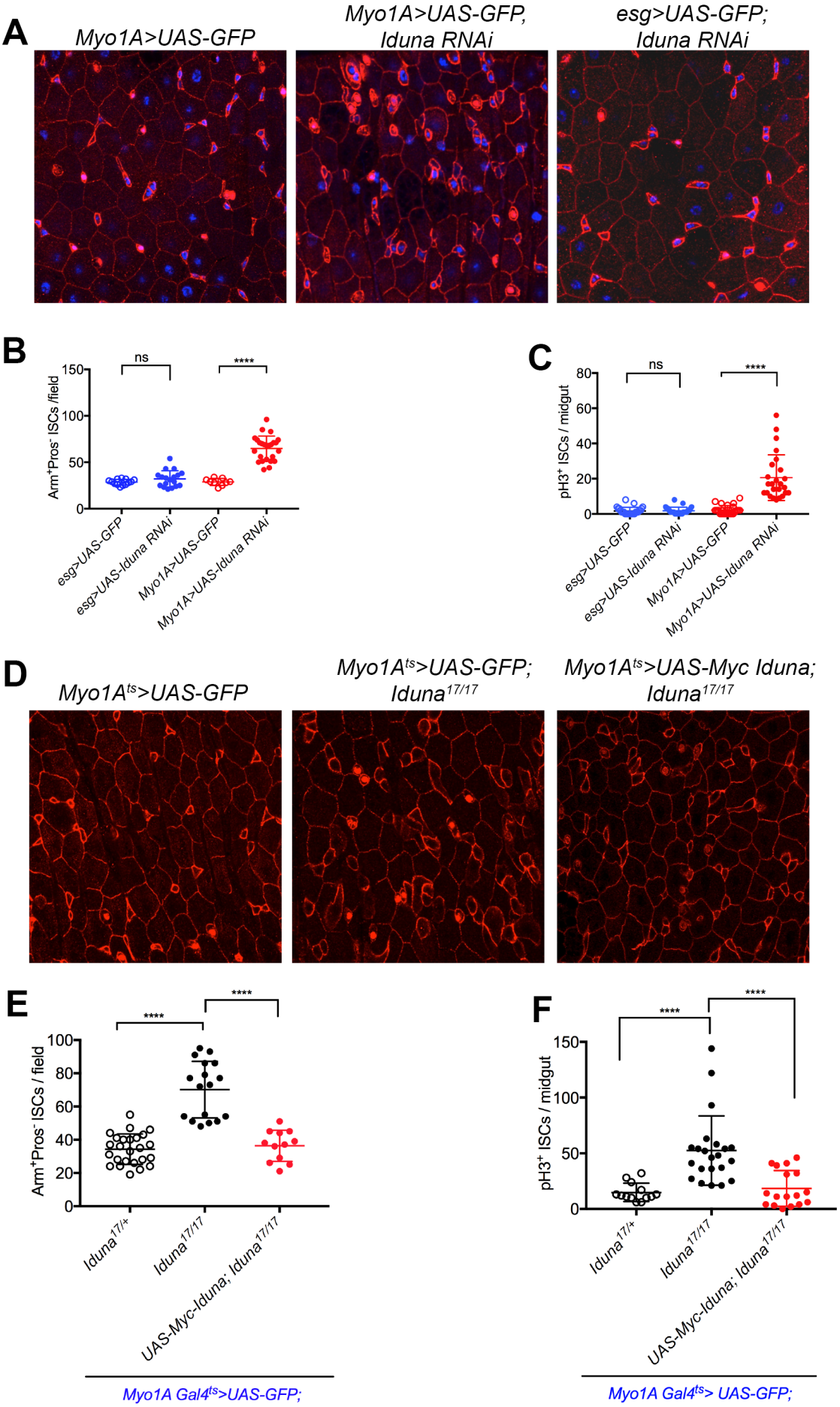
A
Myo1A>UAS-GFP
Myo1A>UAS-GFP, Iduna RNAi
esg>UAS-GFP; Iduna RNAi
B
Arm+Pros- ISCs /field
ns
****
esg>UAS-GFP
esg>UAS-Iduna RNAi
Myo1A>UAS-GFP
Myo1A>UAS-Iduna RNAi
C
pH3+ ISCs / midgut
ns
****
esg>UAS-GFP
esg>UAS-Iduna RNAi
Myo1A>UAS-GFP
Myo1A>UAS-Iduna RNAi
D
Myo1Ats>UAS-GFP
Myo1Ats>UAS-GFP; Iduna17/17
Myo1Ats>UAS-Myc Iduna; Iduna17/17
E
Arm+Pros- ISCs / field
****
****
Iduna17/+
Iduna17/17
UAS-Myc-Iduna; Iduna17/17
Myo1A Gal4ts>UAS-GFP;
F
pH3+ ISCs / midgut
****
****
Iduna17/+
Iduna17/17
UAS-Myc-Iduna; Iduna17/17
Myo1A Gal4ts> UAS-GFP;

Figure 7

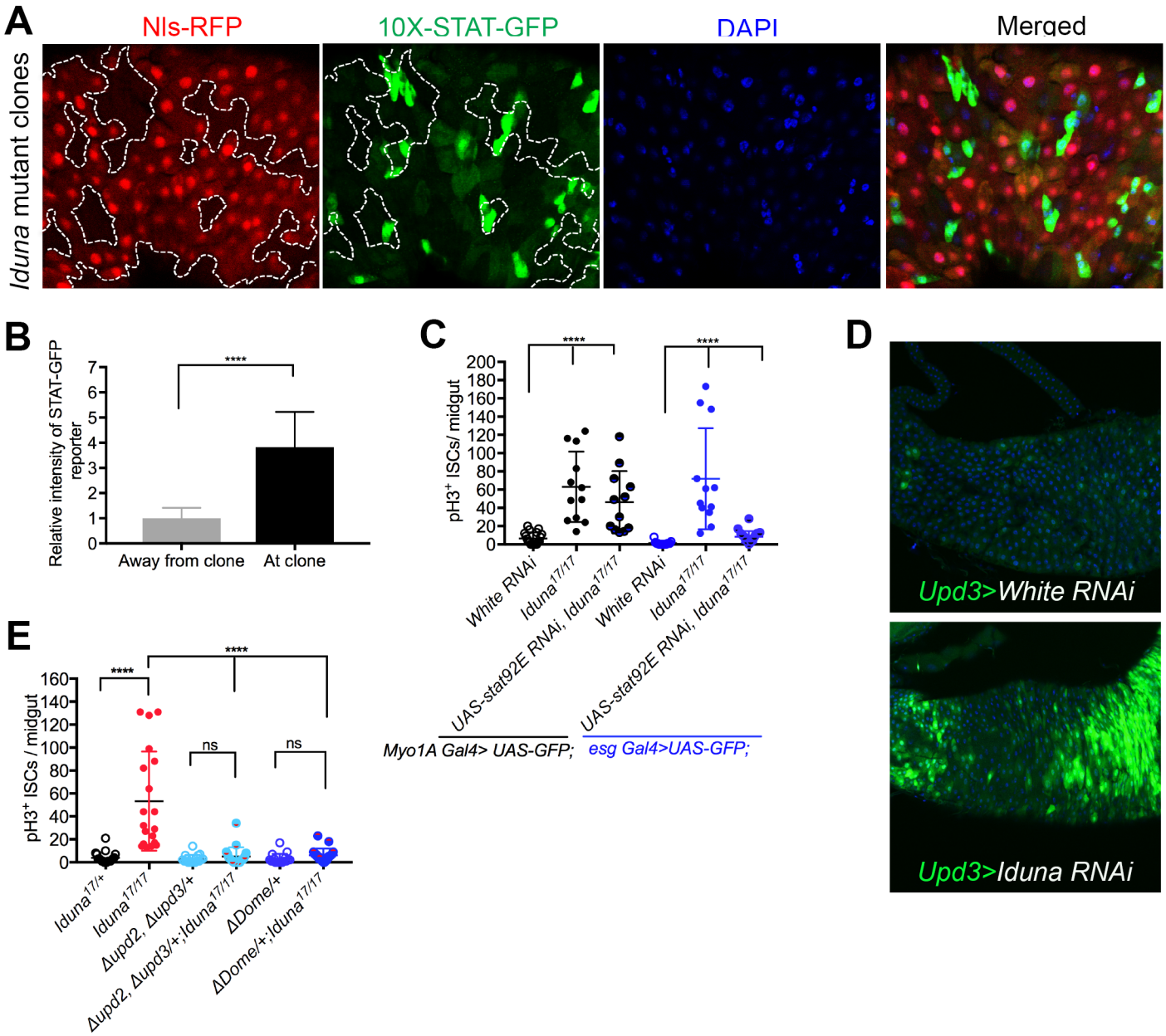
A
Nls-RFP
10X-STAT-GFP
DAPI
Merged
Iduna mutant clones
B
Relative intensity of STAT-GFP reporter
Away from clone
At clone
C
pH3+ ISCs/ midgut
White RNAi
Iduna17/17
UAS-stat92E RNAi; Iduna17/17
Myo1A Gal4> UAS-GFP;
esg Gal4>UAS-GFP;
D
Upd3>White RNAi
Upd3>Iduna RNAi
E
pH3+ ISCs / midgut
Iduna17/+
Iduna17/17
Δupd2, Δupd3/+
Δupd2, Δupd3/+;Iduna17/17
ΔDome/+
ΔDome/+;Iduna17/17
ns

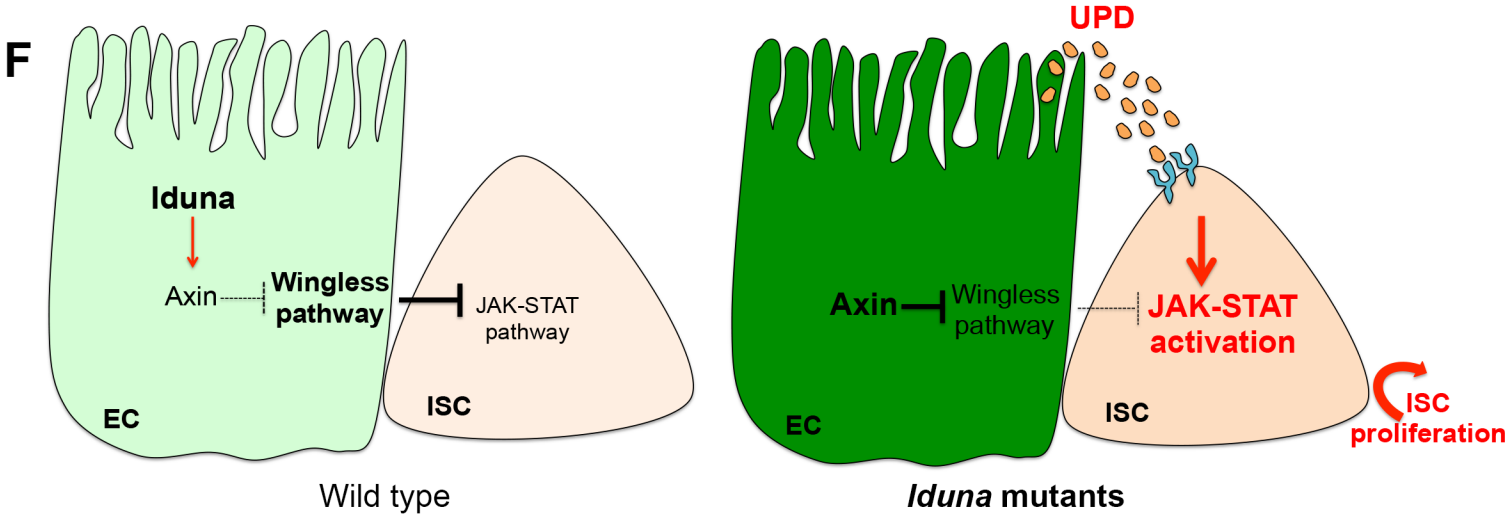
F
Iduna
Axin
Wingless pathway
JAK-STAT pathway
EC
ISC
Wild type
UPD
Axin
Wingless pathway
JAK-STAT activation
ISC proliferation
Iduna mutants

Figure S1

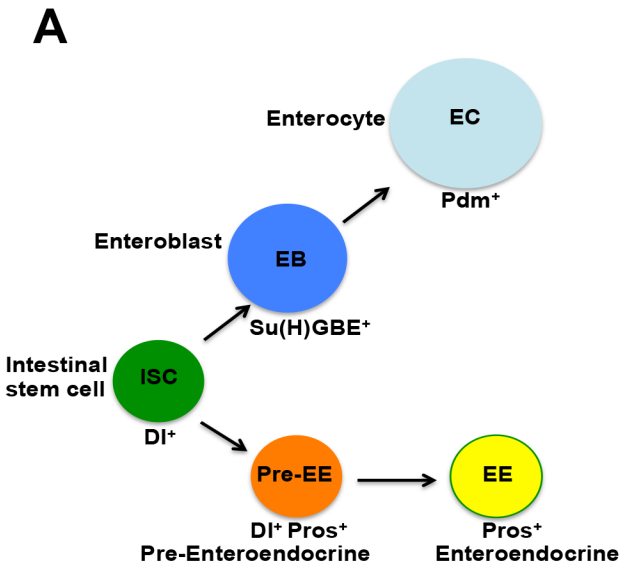
A
Enterocyte
EC
Pdm+
Enteroblast
EB
Su(H)GBE+
Intestinal stem cell
ISC
Dl+
Pre-EE
Dl+ Pros+
Pre-Enteroendocrine
EE
Pros+
Enteroendocrine

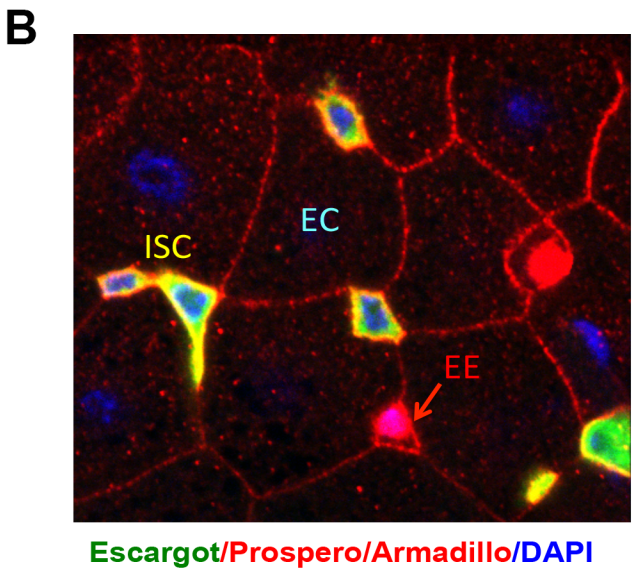
B
ISC
EC
EE
Escargot/Prospero/Armadillo/DAPI

Figure S2

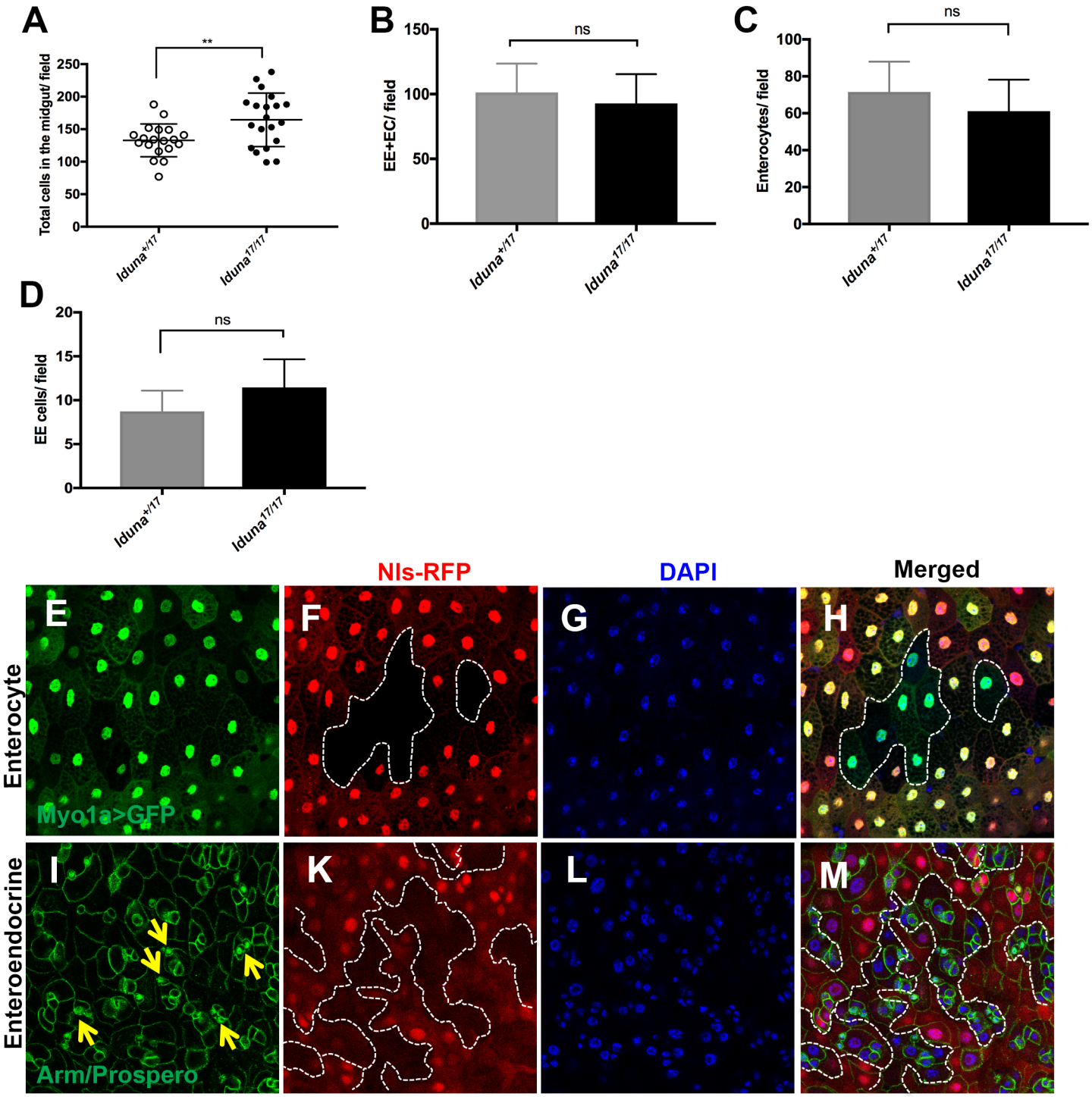
A
Total cells in the midgut/ field
250
200
150
100
50
0
**
Iduna+/17
Iduna17/17
B
EE+EC/ field
150
100
50
0
ns
Iduna+/17
Iduna17/17
C
Enterocytes/ field
100
80
60
40
20
0
ns
Iduna+/17
Iduna17/17
D
EE cells/ field
20
15
10
5
0
ns
Iduna+/17
Iduna17/17
NIs-RFP
DAPI
Merged
Enterocyte
Enteroendocrine
E
F
G
H
I
K
L
M
Myo1a>GFP
Arm/Prospero